Order online now!

www.rockland.com
tech@rockland.com
+1 484.791.3823

Datasheet for 00-8800-25

TrueBlot® Anti-Rabbit Ig IP Agarose Beads

Overview

Description:	TrueBlot® Anti-Rabbit Ig IP Agarose Beads - 00-8800-25
Item No.:	00-8800-25
Size:	2.5 mL
Applications:	IP, SDS-PAGE, WB, ChIP, Other
Reactivity:	Rabbit
Host Species:	Goat

Product Details

Background:	TrueBlot® Anti-Rabbit Ig IP Agarose Beads are a suspension of activated agarose beads coupled with goat Anti-rabbit IgG. It is suitable for precipitation of rabbit IgGs used as the primary antibodies in immunoprecipitation assays. The beads are in suspension and will settle upon storage. Prior to use, mix the vial gently (do not vortex) to ensure delivery of proper bead volume.
Synonyms:	Anti-Rabbit Immunoglobulin Gamma, Agarose-conjugated IgG, Gt-a-Rb IgG, Goat-anti-Rabbit IgG, TrueBlot for immunoprecipitation, IP beads for TrueBlot, Anti-Rabbit IgG IP agarose
Host Species:	Goat
Conjugate:	Agarose ULTRA
Clonality:	Polyclonal
Format:	IgG
Detection Kit Type:	Immunoprecipitation Kit

Target Details

Reactivity:	Rabbit
Purity/Specificity:	TrueBlot® Anti-Rabbit Ig IP Agarose Beads have been tested in SDS-Page, immunoprecipitation, and western blot.
Relevant Links:	• TrueBlot Rabbit IP Set Protocol • SDS

Application Details

Tested Applications:	IP, SDS-PAGE, WB
Suggested Applications:	ChIP, Other (Based on references)
Application Note:	Upon initial use of this product, we recommend that the vial be inverted several times to get the beads into suspension. We recommend using a large bore pipet to pipet up the liquid for use. For storage of the opened vial, we recommend that the vial cap be sealed with parafilm to help prevent evaporation of the buffer. Procedure: Preparation of Immunoprecipitated Sample for SDS-PAGE: 1. Preclear cell lysate: Add 50 µL of Anti-Rabbit IgG Beads and 500µl of cell lysate sample to a microcentrifuge tube and incubate on ice for 30 minutes. Spin at 10,000xg for 3 minutes and transfer the supernatant to a new microcentrifuge tube. 2. Immunoprecipitation: Add 5 µg of primary antibody to the microcentrifuge tube containing the precleared lysate. Incubate on ice for 1 hour. Add 50 µL of Anti-Rabbit IgG Beads. Incubate for 1 hour on a rocking platform. Spin the microcentrifuge tube at 10,000xg for 1 minute. Remove supernatant completely and wash the (pelleted) beads 3 times with 500 µL of Lysis Buffer (50mM Tris HCl, pH 8.0; 150mM NaCl; 1% NP-40). 3. Prepare sample for SDS-PAGE: After the last wash, aspirate supernatant, and add 50 µL Laemmli Buffer (with 50 mM DTT or 2% β-mercaptoethanol, final) to bead pellet. Vortex and heat to 90-100 °C for 10 minutes. Spin at 10,000xg for 3 minutes, collect supernatant, and load onto the gel. Avoid loading Anti-Rabbit Ig Beads. Note: The supernatant can be stored at -20 °C for future use. After thawing, add fresh dithiothreitol and heat as above. Centrifuge the sample at 10,000xg for 1 minute in a microcentrifuge tube to pellet any Anti-Rabbit Ig Beads and immediately transfer an aliquot of the supernatant to gel wells.
Assay Dilutions:	All assays should be optimized by the user. Recommended dilutions (if any) may be listed below.
ChIP:	User Optimized
IP:	TrueBlot anti-Rabbit Ig IP Beads (binds 2.5 mg Ig/ml beads) have been reported for use in IP
WB:	Use with Rabbit TrueBlot® (cat # 18-8816-33)

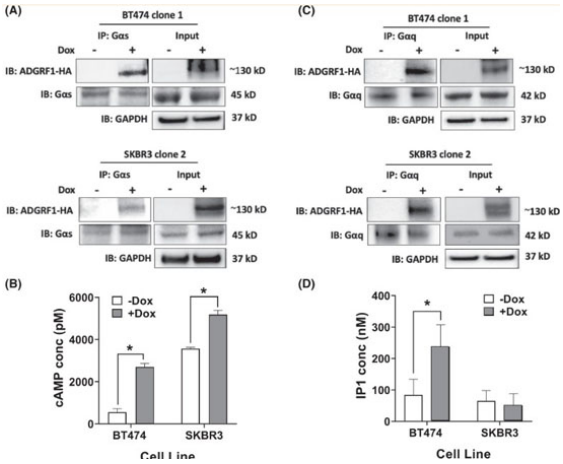
Formulation

Physical State:	Suspension of agarose beads
Concentration:	27.5 mg/cc antibody per cc agarose
Buffer:	0.01 M Sodium Phosphate, 0.15 M Sodium Chloride, pH 7.2
Preservative:	0.09% (w/v) Sodium Azide
Stabilizer:	None

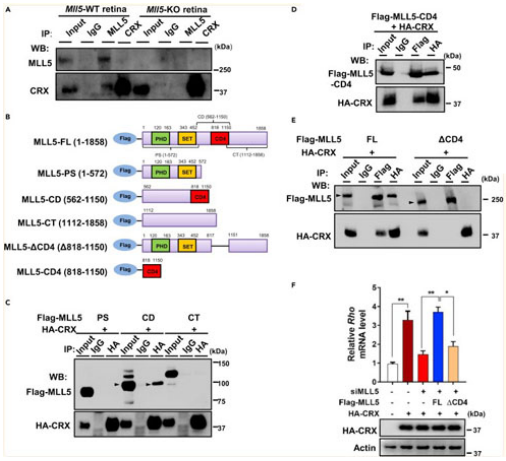
Shipping & Handling

Shipping Condition:	Wet Ice
Storage Condition:	Store vial at 4 °C prior to opening. DO NOT FREEZE.
Expiration:	Expiration date is six (6) months from date of receipt.

Images



Immunoprecipitation
ADGRF1 overexpression activates Gαs/Gαq pathways. BT474 clone 1 and SKBR3 clone 2 were grown in absence (−) or presence (+) of doxycycline (Dox). A, Co-immunoprecipitation with anti-Gαs and immunoblotting with anti-HA indicate that ADGRF1 couples to Gαs in both BT474 and SKBR3. B, Basal levels of cAMP were significantly increased upon ADGRF1 overexpression with Dox in both cells. C, Co–immunoprecipitation with anti-Gαq and immunoblotting with anti-HA indicate that ADGRF1 couples also to Gαq in both cells. D, Basal levels of IP1 were significantly increased upon ADGRF1 overexpression with Dox in BT474 but not SKBR3 cells. *indicates statistically significant difference $P < .05$ by unpaired t test ($N = 3–4$). FIGURE 5. PMID: 34110646.



Immunoprecipitation

MLL5 interacts with CRX via its CD4 domain

(A) Interaction between endogenous MLL5 and CRX. Equivalent amounts of retinal lysates from Mll5-WT or Mll5-KO mice were immunoprecipitated with anti-MLL5 antibody, anti-CRX or normal rabbit IgG, followed by western blotting detection.

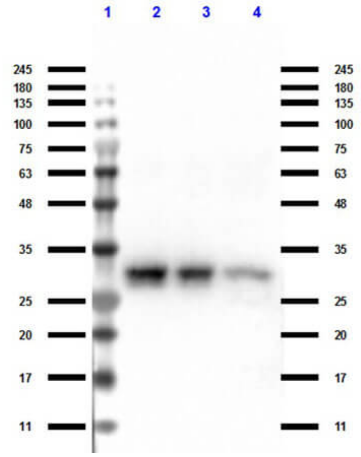
(B) Schematic representation of MLL5 truncated mutants. PS, PHD/SET domain; CD, central domain; CT, C-terminal domain. ΔCT4, deleted CT4 domain.

(C) MLL5 central domain (MLL5-CD) binding to CRX. HEK293T cells expressing HA-CRX together with Flag-MLL5-PS, Flag-MLL5-CD, or Flag-MLL5-CT were subjected to immunoprecipitation with the indicated antibodies followed by western blotting detection.

(D) Interaction between MLL5-CD4 and CRX. HEK293T cells expressing HA-CRX and Flag-MLL5-CD4 were immunoprecipitated with anti-HA antibodies and detected by anti-Flag and anti-HA antibodies.

(E) Depletion of MLL5 CD4 compromises MLL5 interaction with CRX. HEK293T cells expressing HA-CRX along with Flag-MLL5-FL or Flag-MLL5-ΔCD4 were immunoprecipitated with anti-HA and anti-Flag antibodies followed by western blotting detection.

(F) MLL5-ΔCD4 was less potent than MLL5-WT at rescuing transcription of Rho. qPCR analysis of Rho transcript in 661W (CRX OE) cells transfected with MLL5-siRNA (siMLL5) followed by transduction with the indicated lentivirus. Rho expression was normalized to the expression of Tbp. Error bars represent SEM (n = 3), ⍰⍰p < 0.01, Student's t test. Results in (A–F) are representative of at least three experimental repeats. Fig 4. PMID: 35359806.



Western Blot
Western Blot of TrueBlot® Anti-Rabbit Ig IP Agarose Beads. Lane 1: Protein Standard Opal Pre-stained (p/n MB-210-0500). Lane 2: Rb-a-GFP Input. Lane 3: Rb-a-GFP Unbound. Lane 4: Rb-a-Elute. Primary Antibody: TrueBlot® Anti-Rabbit Ig IP Agarose Beads (00-8800-25) at 1 µg/mL for overnight at 4℃. Secondary Antibody: TrueBlot® Rabbit Secondary HRP Antibody (p/n 18-8816-33) at 1:10,000 for 30 min at RT. Block: MB-070 at RT for 30 min. Predicted/Observed size: 27 kDa.

References

- Satapathy SR et al. Nuclear PD-L1 regulates YAP-driven transcription via the PGE2-EP4-YAP-importin α3 axis in solid tumors. *Cell Rep.* (2026)
- Hamaidi I et al. SIRT2-mediated deacetylation of LCK governs the magnitude of T cell receptor signaling. *Nat Immunol.* (2026)
- Tseng-Rogenski SS et al. Inflammation Drives Phosphorylation and Acetylation of MutS Homolog 3 and Interaction with Cytosolic HDAC6. *Cancer.* (2026)
- Gao J et al. Dual roles of USP1 in HELLS deubiquitination and SUMOylation drive EMT and FOLFOX-based chemoresistance. *Oncogenesis.* (2025)
- Luo J et al. SLC15A3 plays a crucial role in pulmonary fibrosis by regulating macrophage oxidative stress. *Cell Death Differ.* (2024)
- Zhou Q et al. Response to: Energy sensor AMPKγ does not exist in isolation from AMPKα or interact with PPP6C in muscle and liver from humans and mice *Mol Cell.* (2024)
- Schafer CM. et al. Cytokine-Mediated Degradation of the Transcription Factor ERG Impacts the Pulmonary Vascular Response to Systemic Inflammatory Challenge. *bioRxiv Preprint.* (2023)
- Roldán-Romero JM et al. Deubiquitinase USP9X loss sensitizes renal cancer cells to mTOR inhibition. *Int J Cancer.* (2023)
- Schafer CM et al. Cytokine-Mediated Degradation of the Transcription Factor ERG Impacts the Pulmonary Vascular Response to Systemic Inflammatory Challenge. *Arterioscler Thromb Vasc Biol.* (2023)
- Coppola V et al. The autophagic protein FYCO1 controls TNFRSF10/TRAIL receptor induced apoptosis and is inactivated by CASP8 (caspase 8) *Autophagy* (2023)
- Aso M et al. First-in-human autologous implantation of genetically modified adipocytes expressing LCAT for the treatment of familial LCAT deficiency. *Heliyon.* (2022)
- Zhang X et al. MLL5 is involved in retinal photoreceptor maturation through facilitating CRX-mediated photoreceptor gene transactivation. *iScience.* (2022)

- Abdulkareem, NM et al. A novel role of ADGRF1 (GPR110) in promoting cellular quiescence and chemoresistance in human epidermal growth factor receptor 2-positive breast cancer. *Faseb Journal : Official Publication of the Federation of American Societies for Experimental Biology* (2021)
- Zheng X. et al. Upregulation of OATP1A2 in human oesophageal squamous cell carcinoma cells via the HDAC6-GCN5/PCAF-H3K9Ac axis. *Xenobiotica.* (2021)
- Nassal DM et al. Ca2+/calmodulin kinase II–dependent regulation of βIV-spectrin modulates cardiac fibroblast gene expression, proliferation, and contractility. *J Biol Chem.* (2021)
- Rodriguez GY et al. PFTK1 kinase regulates axogenesis during development via RhoA activation. *bioRxiv Preprint* (2021)
- Alvandi Z., Opas M. c-Src kinase inhibits osteogenic differentiation via enhancing STAT1 stability. *PLoS One* (2020)
- Chu CS et al. Unique Immune Cell Coactivators Specify Locus Control Region Function and Cell Stage. *Mol Cell* (2020)
- Zheng JP et al. YY1 directly interacts with myocardin to repress the triad myocardin/SRF/CArG box-mediated smooth muscle gene transcription during smooth muscle phenotypic modulation. *Sci Rep.* (2020)
- Yi SA. et al. Fermented ginseng extract, BST204, disturbs adipogenesis of mesenchymal stem cells through inhibition of S6 kinase 1 signaling. *J Ginseng Res.* (2020)
- Akiyama H. et al. Control of cell migration by the novel protein phosphatase-2A interacting protein inka2. *Cell Tissue Res.* (2020)
- Weiterer SS, Meier-Soelch J, Georgomanolis T, et al. Distinct IL-1α-responsive enhancers promote acute and coordinated changes in chromatin topology in a hierarchical manner. *EMBO J.* (2020)
- Rueda EM, Hall BM, Hill MC, et al. The Hippo Pathway Blocks Mammalian Retinal Müller Glial Cell Reprogramming. *Cell Rep.* (2019)
- Amano H et al. Telomere Dysfunction Induces Sirtuin Repression that Drives Telomere-Dependent Disease. *Cell Metab.* (2019)
- Zhu Q et al. Regulation of OCT2 transcriptional repression by histone acetylation in renal cell carcinoma. *Epigenetics* (2019)
- Chern YJ et al. The interaction between SPARC and GRP78 interferes with ER stress signaling and potentiates apoptosis via PERK/eIF2α and IRE1α/XBP-1 in colorectal cancer. *Nature* (2019)
- Mayr-Buro C et al. Single-Cell Analysis of Multiple Steps of Dynamic NF-κB Regulation in Interleukin-1α-Triggered Tumor Cells Using Proximity Ligation Assays. *Cancers (Basel)* (2019)
- Sciuto MR et al. Two-Step Coimmunoprecipitation (TIP) Enables Efficient and Highly Selective Isolation of Native Protein Complexes. *Mol Cell Proteomics* (2018)
- Logan C et al. Functional role for stable microtubules in lens fiber cell elongation. *Exp Cell Res* (2018)
- Scheri K et al. c-MET receptor as potential biomarker and target molecule for malignant testicular germ cell tumors. *Oncotarget* (2018)
- Moriya et al. PRDM14 directly interacts with heat shock proteins HSP90α and glucose-regulated protein 78. *Cancer Science* (2018)
- Cervin et al. GM1 ganglioside-independent intoxication by Cholera toxin. *PLOS Pathogens* (2018)

- Peña-Philippides et al. Inhibition of MicroRNA-155 Supports Endothelial Tight Junction Integrity Following Oxygen-Glucose Deprivation. *Journal of the American Heart Association* (2018)
- Tykesson E, Hassinen A, Zielinska K, et al. Dermatan sulfate epimerase 1 and dermatan 4-O-sulfotransferase 1 form complexes that generate long epimerized 4-O-sulfated blocks. *J Biol Chem.* (2018)
- Scheri, KC et al. c-MET receptor as potential biomarker and target molecule for malignant testicular germ cell tumors. *Oncotarget* (2018)
- Zhai et al. NLRP1 promotes tumor growth by enhancing inflammasome activation and suppressing apoptosis in metastatic melanoma. *Oncogene* (2017)
- Emmett et al. Histone deacetylase 3 prepares brown adipose tissue for acute thermogenic challenge. *Nature* (2017)
- Armour et al. An HDAC3-PROX1 corepressor module acts on HNF4α to control hepatic triglycerides. *Nature Communications* (2017)
- Lee et al. An ID2-dependent mechanism for VHL inactivation in cancer. *Nature* (2016)
- Wang et al. Skin Keratins. *Methods in Enzymology* (2016)
- Whitt et al. BK channel inactivation gates daytime excitability in the circadian clock. *Nature Communications* (2016)
- Hwang et al. Leucine Carboxyl Methyltransferase 1 (LCMT-1) Methylates Protein Phosphatase 4 (PP4) and Protein Phosphatase 6 (PP6) and Differentially Regulates the Stable Formation of Different PP4 Holoenzymes. *Journal of Biological Chemistry* (2016)
- Jabir et al. Mitochondrial damage contributes to Pseudomonas aeruginosa activation of the inflammasome and is downregulated by autophagy. *Autophagy* (2015)
- Wands AM et al. Fucosylation and protein glycosylation create functional receptors for cholera toxin. *Elife* (2015)
- Sugawara S, Ito T, Sato S, et al. Generation of aminoterminally truncated, stable types of bioactive bovine and porcine fibroblast growth factor 4 in Escherichia coli. *Biotechnol Appl Biochem.* (2015)
- Basu S et al. Suppression of MAPK/JNK-MTORC1 signaling leads to premature loss of organelles and nuclei by autophagy during terminal differentiation of lens fiber cells. *Autophagy* (2014)
- Nicholas C et al. PRMT5 is upregulated in malignant and metastatic melanoma and regulates expression of MITF and p27 (Kip1.) *PLoS One* (2013)
- Gao Y, Koppen A, Rakhshandehroo M, et al. Early adipogenesis is regulated through USP7-mediated deubiquitination of the histone acetyltransferase TIP60. *Nat Commun.* (2013)
- Rzeczkowski K, Beuerlein K, Müller H, et al. c-Jun N-terminal kinase phosphorylates DCP1a to control formation of P bodies. *J Cell Biol.* (2011)
- View More ...

Disclaimer

This product is for research use only and is not intended for therapeutic or diagnostic applications. Please contact a technical service representative for more information. All products of animal origin manufactured by Rockland Immunochemicals are derived from starting materials of North American origin. Collection was performed in United States Department of Agriculture (USDA) inspected facilities and all materials have been inspected and certified to be free of disease and suitable for exportation. All properties listed are typical characteristics and are not specifications. All suggestions and data are offered in good faith but without guarantee as conditions and methods of use of our products are beyond our control. All claims must be made within 30 days following the date of delivery. The prospective user must determine the suitability of our materials before adopting them on a commercial scale. Suggested uses of our products are not recommendations to use our products in violation of any patent or as a license under any patent of Rockland Immunochemicals, Inc. If you require a commercial license to use this material and do not have one, then return this material, unopened to: Rockland Inc., P.O. BOX 5199, Limerick, Pennsylvania, USA.